Optimal phase-based control of strongly perturbed limit cycle oscillators using phase reduction techniques

Adharaa Neelim Dewanjee◉ and Dan Wilson[*]

Department of Electrical Engineering and Computer Science, University of Tennessee, Knoxville, Tennessee 37996, USA

Phase reduction is a well-established technique for analysis and control of weakly perturbed limit cycle oscillators. However, its accuracy is diminished in a strongly perturbed setting where information about the amplitude dynamics must also be considered. In this paper, we consider phase-based control of general limit cycle oscillators in both weakly and strongly perturbed regimes. For use at the strongly perturbed end of the continuum, we propose a strategy for optimal phase control of general limit cycle oscillators that uses an adaptive phase-amplitude reduced order model in conjunction with dynamic programming. This strategy can accommodate large magnitude inputs at the expense of requiring additional dimensions in the reduced order equations, thereby increasing the computational complexity. We apply this strategy to two biologically motivated prototype problems and provide direct comparisons to two related phase-based control algorithms. In situations where other commonly used strategies fail due to the application of large magnitude inputs, the adaptive phase-amplitude reduction provides a viable reduced order model while still yielding a computationally tractable control problem. These results highlight the need for discernment in reduced order model selection for limit cycle oscillators to balance the trade-off between accuracy and dimensionality.

I. INTRODUCTION

Periodic oscillations are commonly observed in a wide array of applications spanning the physical, chemical, and biological sciences [1]. Due to the sheer size and complexity of many oscillatory systems, model order reduction is often a necessary first step for mathematical analysis and control design. Phase reduction [1–3] is a widely used tool for model-order reduction of limit cycle oscillators, transforming systems of the form

$$\dot{x} = F(x) + U(t), \tag{1}$$

where $x \in \mathbb{R}^N$ is the system state, F describes the unperturbed dynamics, and U is an exogenous perturbation to a one-dimensional system,

$$\dot{\theta} = \omega + Z^T(\theta)U(t), \tag{2}$$

where $\theta \in [0, 2\pi)$ represents the oscillator's phase, ω is the unperturbed natural frequency, $Z(\theta)$ is the phase response curve that captures the response to external inputs, and ^{T} denotes the transpose. Phase reduction greatly reduces the dimension of the original system by viewing the dynamics not in terms of the underlying state but rather in terms of the timing of oscillations. This, in turn, often allows for a numerically tractable formulation and solution of optimal control problems [4–6] and an elegant characterization of emergent behaviors in weakly coupled oscillator networks [7–10].

The phase reduction (2) implicitly assumes that the system state is close to the underlying periodic orbit [3]. As such, it

is only valid in the limit that $U(t)$ is small—large inputs that drive the system far from the limit cycle will invalidate these underlying assumptions. The largeness of $U(t)$ is considered relative to the nonunity Floquet multipliers of the periodic orbit [11]. Particularly, when some of these Floquet multipliers are near 1 (indicating slow convergence), the cumulative effect of even small inputs can grow over time ultimately yielding large deviations from the nominal limit cycle. In practice, the effectiveness of a given control algorithm obtained from the reduction (2) but applied to the full model (1) will begin to degrade as the magnitude of inputs becomes larger [5,6,12].

Limitations of the standard phase reduction have prompted the development of new strategies that can consider larger magnitude inputs. Techniques that employ entrainment maps [13,14] consider the dynamic in response to large, periodic perturbations. Related techniques consider the effect of a residual phase response curve [15,16] to account for a slow decay to the periodic orbit that occurs over multiple cycles. Other strategies consider the response to strong inputs in the limit that they change sufficiently slowly [17,18] or rapidly [19]. Noting that $Z(\theta)$ from (2) is the gradient of the phase with respect to the state evaluated on the periodic orbit, a variety of strategies also consider the phase dynamics where this gradient is approximated to high orders of accuracy in a basis of amplitude coordinates [20–23], i.e., that capture the dynamics in directions transverse to the limit cycle.

The use of amplitude coordinates is critical when considering large magnitude perturbations applied to phase oscillators. The isostable coordinate system has recently been proposed for this purpose. Isostable coordinates share a close connection to Koopman operator theory and can be formally defined as level sets of slowly decaying eigenfunctions of the

---

Koopman operator [24,25] at all locations in the basin of attraction of a periodic orbit. To linear orders of accuracy, isostable coordinates give a sense of the distance from the periodic orbit in a basis of Floquet eigenfunctions. By truncating rapidly decaying isostable coordinates and retaining those with slow decay, the standard phase reduction (2) can be augmented with information about isostable coordinates to arrive at a phase-isostable reduction [26]. To leading order of accuracy in the basis of isostable coordinates, the equations are

$$\dot{\theta} = \omega + Z^T(\theta)U(t),$$
$$\dot{\psi}_j = \kappa_j\psi_j + I_j^T(\theta)U(t) \tag{3}$$

for $j = 1, \ldots, \beta$. Here ψ_j represents the jth isostable coordinate with associated Floquet exponent κ_j and isostable response curve $I_j^T(\theta)$. Here, only the β slowest decaying isostable coordinates are retained to arrive at a reduced order system. As compared to Eq. (2), the additional information about the isostable coordinates provided by (3) can be used to guarantee that the reduced order model will provide a good approximation to the full order equations (1) provided the magnitude of $\psi_1, \ldots, \psi_\beta$ remains small. This general approach has been applied successfully to achieve faster entrainment [27] or more accurate phase control [28] than can be obtained with knowledge of the phase dynamics alone.

The phase-amplitude reduction of the form (3) still requires the state to remain close to the underlying limit cycle. In practice, this often represents a significant limitation for control applications. In many cases, the goal of achieving a given control objective and keeping the isostable coordinates small are in direct conflict, resulting in a control problem that cannot be solved. More recently the notion of an adaptive coordinate system has been proposed [29] that considers a continuous family of limit cycles that result when an underlying set of parameters is changed. By adaptively selecting the nominal attractor with the goal of keeping the associated amplitude coordinates low, a very accurate reduced order model can be obtained in regimes for which the standard phase reduction from (2) and the phase-amplitude reduction from (3) fail. However, effective strategies for formulating and solving optimal control problems when using the adaptive phase-amplitude reduction have yet to be investigated.

In this paper, we investigate a general optimal control framework for phase-based control of limit cycle oscillators in a strongly perturbed regime. This strategy considers the adaptive phase-amplitude reduced order modeling approach from Ref. [29] to accommodate large magnitude inputs. We provide direct comparisons to related algorithms that consider phase-only reduced order models of the form (2) and phase-isostable models of the form (3). The organization of this paper is as follows: Section II provides necessary background on the phase-based reduced order modeling strategies considered in this paper. Section III describes the proposed optimal control strategy for rapidly advancing or delaying the phase of a limit cycle oscillator and provide comparisons to previously developed strategies from Refs. [4,27,28]. Section IV applies these control algorithms in two different numerical models: the first considers a model for a population of circadian oscillators and the second considers a model of coupled neurons.

As compared to previously proposed control strategies, the adaptive phase-amplitude model requires the solution of a higher dimensional optimal control problem, but in return can be used to accurately yield larger magnitude shifts to the unperturbed period of oscillation. Section V provides concluding remarks.

II. BACKGROUND

In this paper, we will consider general ordinary differential equations of the form

$$\dot{x} = F(x, p_0) + U(t), \tag{4}$$

where $p_0 \in \mathbb{R}^M$ is a collection of nominal parameters and x, F, and U are defined in the same way as the terms from (1). Suppose that for a fixed value of p_0 and taking $U(t) = 0$, (4) exhibits a stable, T-periodic orbit $x_{p_0}^\gamma$.

A. Phase and phase reduction

Let $\theta \in [0, 2\pi)$ be a phase defined for any $x \in x_{p_0}^\gamma$ and scaled so $d\theta/dt = \omega = 2\pi/T$ for all points on the periodic orbit when $U(t) = 0$. Isochrons can be used to define phase for all states in the basin of attraction of the limit cycle [1,30]. Letting θ_1 denote a phase that corresponds to $w(0) \in x_{p_0}^\gamma$, the θ_1 isochron can be defined as the set of all $v(0)$ such that

$$\lim_{t \to \infty} \|w(t) - v(t)\| = 0, \tag{5}$$

where $\| \cdot \|$ denotes any vector norm. As seen from the definition in (5), the phase, as defined by isochrons, gives information about the asymptotic behavior. Provided that $U(t)$ is sufficiently small in (4), so the state stays close to the limit cycle, phase reduction can be used to analyze the behavior of (4) in the weakly perturbed limit according to

$$\dot{\theta} = \omega(p_0) + Z^T(\theta, p_0)U(t), \tag{6}$$

where $Z(\theta, p_0) \in \mathbb{R}^N$ is the gradient of the phase with respect to the state. It can be useful to work in a phase-reduced coordinate framework because of the reduction in dimensionality from N to one.

B. Reduction framework based on phase and isostable coordinates

Although phase reduction is an effective approach for reducing the complexity of weakly perturbed oscillatory systems, it often fails when large inputs are required. In these cases, it can be useful to augment the phase dynamics with amplitude coordinates that capture the dynamics in directions transverse to the limit cycle. Floquet theory [31] can be used to achieve this goal. Defining $\Delta x = x - x_{p_0}^\gamma(\theta)$ to a linear approximation,

$$\Delta\dot{x} = DF\Delta x, \tag{7}$$

where DF denotes the Jacobian matrix evaluated at $x_{p_0}^\gamma(\theta)$. Noting that DF is T periodic, let Φ be the monodromy matrix, i.e., with the property that $\Delta x(T) = \Phi\Delta x(0)$. Provided Φ is diagonalizable, solutions near the periodic orbit can be

represented according to [32]

$$x - x_{p_0}^\gamma(\theta) = \sum_{j=1}^{N-1} \psi_j g^j(\theta, p_0) + \mathcal{O}(\psi_1^2) + \ldots + \mathcal{O}(\psi_{N-1}^2), \quad (8)$$

where, $\psi_j \in \mathbb{C}$ is an isostable coordinate (identical to Floquet coordinates to a linear approximation) and $g^j(\theta) \in \mathbb{C}^N$ is a corresponding Floquet eigenfunction associated with the periodic orbit $x_{p_0}^\gamma(\theta)$. Note that to linear orders of accuracy, isostable coordinates are identical to Floquet coordinates. Also, the Floquet eigenfunction $g^N(\theta, p_0)$ has been absorbed by the phase coordinate giving $N-1$ total isostable coordinates. To linear orders of accuracy, isostable coordinates can be used to augment the phase dynamics. To linear order, the phase-isostable reduction is

$$\dot{\theta} = \omega(p_0) + Z^T(\theta, p_0)U(t),$$
$$\dot{\psi}_j = \kappa_j(p_0)\psi_j + I_j^T(\theta, p_0)U(t) \quad (9)$$

for $j = 1, \ldots, \beta$. Above, $I_j(\theta, p_0) \in \mathbb{C}^N$ is the gradient of ψ_j with respect to the state evaluated on the periodic orbit and $\kappa_j \in \mathbb{C}$ is a corresponding Floquet exponent. Note that since $x_{p_0}^\gamma$ is assumed to be stable, $\text{Real}(\kappa_j) < 0$ for all j. Additionally, for $j = \beta + 1, \ldots, N-1$, it is assumed that $|\text{Real}(\kappa_j)| = O(1/\epsilon)$, where $0 \ll \epsilon < 1$, so the corresponding value of $\psi_j = O(\epsilon)$, allowing it to be truncated [29]. Intuitively, for any isostable coordinate corresponding to a large magnitude Floquet exponent, the influence of any perturbations will decay rapidly. As a matter of practical implementation, any isostable coordinate ψ_j can typically be truncated for which $|\exp(\kappa_j T)| < 0.2$, i.e., so $|\psi_j(t + T)| < 0.2|\psi_k(t)|$ when taking $U(t) = 0$. To first-order accuracy, the phase dynamics are decoupled from the isostable coordinate dynamics. Expansions taken to higher orders of accuracy in the isostable coordinates can be computed to give more accurate results. For instance, to second-order accuracy in the expansion of isostable coordinates, the dynamics are [22,32]

$$\dot{\theta} = \omega(p_0) + Z^T(\theta, p_0)U(t) + \sum_{k=1}^{\beta} \psi_k B^{k^T}(\theta, p_0)U(t),$$

$$\dot{\psi}_j = \kappa_j(p_0)\psi_j + I_j^T(\theta, p_0)U(t) + \sum_{k=1}^{\beta} \psi_k C_j^{k^T}(\theta, p_0)U(t), \quad (10)$$

where $B^k(\theta, p_0)$ and $C_j^k(\theta, p_0)$ provide second-order corrections for the phase and isostable coordinate dynamics. The interested reader is directed to both Refs. [28,33] for a more complete description of phase-isostable reduction and other phase reduction strategies.

C. Adaptive phase-isostable reduction

When large magnitude inputs are applied that drive the state of (4) far from the underlying periodic orbit $x_{p_0}^\gamma(\theta)$, phase-only (5) and phase-isostable reduction (9) generally fail. For control applications that require large magnitude inputs, the adaptive phase-isostable strategy [29] can be a viable alternative. Instead of considering a reduced order

model with respect to a single periodic orbit $x_{p_0}^\gamma$, the adaptive phase-isostable approach considers a family of periodic orbits that emerge for different constant parameter sets. To this end, suppose that for any $p \in P \subseteq \mathbb{R}^M$, $\dot{x} = F(x, p)$ admits a stable periodic orbit x_p^γ. Phase and isostable coordinates can be defined for each orbit to yield an extended phase $\theta(x, p)$ and extended isostable coordinates $\psi_1(x, p), \ldots, \psi_\beta(x, p)$ that correspond to the state on the p-limit cycle. As discussed in Ref. [29], the phase on each limit cycle can be disambiguated by defining a level set to correspond to the crossing of some Poincaré section. To proceed, as described in Ref. [29], we can consider a slightly modified version of Eq. (4)

$$\dot{x} = F(x, p) + U_e(x, t, p), \quad (11)$$

where

$$U_e(x, t, p) = U(t) + F(x, p_0) - F(x, p). \quad (12)$$

Equation (11) above is identical to (4), but can be used to consider the system dynamics relative to any periodic orbit x_p^γ for $p \in P$. Particularly, if p can be chosen dynamically to keep the associated isostable coordinates small, the reduced order model can be used to accurately characterize the response to large magnitude inputs. Allowing p to be nonstatic, transformation to phase and isostable coordinates gives

$$\frac{d\theta}{dt} = \frac{\partial\theta}{\partial x} \cdot \frac{dx}{dt} + \frac{\partial\theta}{\partial p} \cdot \frac{dp}{dt},$$
$$\frac{d\psi_j}{dt} = \frac{\partial\psi_j}{\partial x} \cdot \frac{dx}{dt} + \frac{\partial\psi_j}{\partial p} \cdot \frac{dp}{dt} \quad (13)$$

for $j = 1, \ldots, \beta$. Similar to the formulation from (8), it is assumed that $\min_{p, j > \beta}(|\text{Real}(\kappa_j(p))|) = O(1/\epsilon)$ so these $N - 1 - \beta$ rapidly decaying isostable coordinates can be truncated [29]. Note that above, for instance, the notation $\frac{\partial}{\partial x}$ denotes the partial derivative with respect to x and $\frac{d}{dt}$ denotes the total derivative with respect to time. When the isostable coordinates are small and p is held constant, the phase and isostable dynamics were already given by Eq. (9), so $\frac{\partial\theta}{\partial x} \cdot \frac{dx}{dt} = \omega(p) + Z^T(\theta, p)U_e$ and $\frac{\partial\psi_j}{\partial x} \cdot \frac{dx}{dt} = \kappa_j(p)\psi_j + I_j^T(\theta, p)U_e$. As discussed in Ref. [29], the remaining terms are given by

$$D(\theta, p) \equiv \frac{\partial\theta}{\partial p} = -Z(\theta, p) \cdot \frac{\partial x_p^\gamma}{\partial p_1} \cdots - Z(\theta, p) \cdot \frac{\partial x_p^\gamma}{\partial p_M}^T,$$

$$Q_j(\theta, p) \equiv \frac{\partial\psi_j}{\partial p} = -I_j(\theta, p) \cdot \frac{\partial x_p^\gamma}{\partial p_1} \ldots - I_j(\theta, p) \cdot \frac{\partial x_p^\gamma}{\partial p_M}^T, \quad (14)$$

where $\partial x_p^\gamma/\partial p_i|_{\theta_0} \equiv \lim_{a \to 0}(x_{p+e_i a}^\gamma(\theta_0) - x_p^\gamma(\theta_0))/a$, where e_i is the ith component of the standard unit basis (i.e., the change in the stable periodic orbit in response to a change in the parameter p_i). The adaptive phase-isostable reduction is obtained by substituting (14) into (13) together with the phase and isostable dynamics from (9).

$$\dot{\theta} = \omega(p) + Z(\theta, p) \cdot U_e(x, t, p) + D(\theta, p) \cdot \dot{p},$$
$$\dot{\psi}_j = \kappa_j(p)\psi_j + I_j(\theta, p) \cdot U_e(x, t, p) + Q_j(\theta, p) \cdot \dot{p},$$
$$\dot{p} = G_p(p, \theta, \psi_1, \ldots, \psi_\beta), \quad (15)$$

where $j = 1, \ldots, \beta$ and the goal of the function G_p is to actively select p (and consequently $\dot{p}$) in a way that minimizes the isostable coordinates. Note that higher accuracy representations can be used for $\frac{\partial \theta}{\partial x} \cdot \frac{dx}{dt}$ and $\frac{\partial \psi_j}{\partial x} \cdot \frac{dx}{dt}$, for instance, using Eq. (10) instead of (9), ultimately yielding a slightly different form for (15).

As a matter of practical implementation, there is a large degree of flexibility in the choice of the adaptive parameter p. In control applications, it is often useful to choose p to be similar to the applied input, however, this is not an absolute requirement. The dynamics of p in Eq. (15) as governed by G_p can be chosen freely with the requirement that $\psi_1, \ldots, \psi_\beta$ remain small at all times. Reference [29] discusses some heuristics for choosing G_p that are valid in specific circumstances, but there is no general way of accomplishing this task. In this paper, we consider strategies for determining G_p through the formulation and solution of an optimal control problem. Note that because the reductions (9) and (10) are similar to adaptive phase-isostable reduction but do not consider the nonstatic parameter set, they will be referred to as nonadaptive phase-isostable reduced order equations in this paper.

III. OPTIMAL PHASE CONTROL WITH DIFFERENT REDUCED ORDER MODELS

In this paper, we are interested in general phase-based control of limit cycles in response to strong inputs. To this end, we consider a prototype problem of modifying the period of a limit cycle oscillator of the form (4) using an external input $U(t)$. Specifically, we consider an initial condition $x_0 \in x_{p_0}^\gamma$ with initial phase $\theta(x_0) = 0$ and seek a minimum energy input $U(t)$ that yields a final phase $\theta = 2\pi$ at time $t = T_1$ (i.e., so the oscillator completes one full oscillation in the interval $t \in [0, T_1]$). To simplify the problem, we assume that

$$U(t) = hu(t), \qquad (16)$$

where $h \in \mathbb{R}^N$ so $U(t)$ is a rank-1 input. Also, for simplicity of exposition, when considering the adaptive phase-isostable reduction we let $p \in \mathbb{R}$ and note that it would be straightforward to consider more parameters in the problem formulation.

We formulate an optimal control problem in discrete time using a dynamic programming approach [34,35] when using either the phase-only reduced order equations (6), nonadaptive phase-isostable reduced order equations (9), and adaptive phase-isostable reduced order equations (15) to inform the phase dynamics, mapping from one state to the next using a forward Euler scheme with time step $\Delta t = T_1/\eta$, where η is the total number of time steps considered in the optimization. We consider a control space $\mathcal{U} \in [u_{\min}, u_{\max}]$. Also, for the adaptive reduction, we consider an adaptive parameter space $\mathcal{P} \in [p_{\min}, p_{\max}]$ which sets the range of the adaptive parameters. As a brief technical note, we did consider other strategies such as calculus of variations and Hamilton-Jacobi-Bellman approaches [35] for solution of this control problem in continuous time. Ultimately, these continuous time approaches were unsuccessful due to the relatively high dimension of the resulting control problem when considering the adaptive phase-isostable reduction.

A. Problem formulation when using the adaptive phase-isostable reduction

Towards a description of the optimization problem when using the adaptive phase-isostable reduction (15), we consider the following difference equation:

$$
\begin{aligned}
\theta_{k+1} &= [\omega(p_k) + Z(\theta_k, p_k) \cdot U_e(\theta_k, p_k, u_k) \\
&\quad + D(\theta_k, p_k)v_k]\Delta t + \theta_k, \\
\psi_{j,k+1} &= [\kappa_j(p_k)\psi_{j,k} + I_j(\theta_k, p_k) \cdot U_e(\theta_k, p_k, u_k) \\
&\quad + Q_j(\theta_k, p_k)v_k]\Delta t + \psi_{j,k}, \quad j = 1, \ldots, \beta, \\
p_{k+1} &= p_k + v_k\Delta t,
\end{aligned}
\qquad (17)
$$

where k is the time step, $u_k \in \mathcal{U}$, and $v_k \in \mathbb{R}$ which controls the update on the adaptive parameter and is constrained so $p_{k+1} \in \mathcal{P}$. Note that in the above formulation, we assume that $\psi_1, \ldots, \psi_\beta$ is small so the state $x \approx x_{p_k}^\gamma(\theta)$, allowing U_e to be written as a function of u, θ, and p. Also, while Eq. (17) considers accuracy of the phase and isostable coordinate to first order in the expansion of isostable coordinates, higher order terms can also be added, e.g., using (10) instead of (9).

Recall that the goal is to identify an energy efficient input that causes the oscillator to complete one full oscillation on the interval $t \in [0, T_1]$. Towards this goal, letting $\theta_1 = \psi_{1,1} = \cdots = \psi_{\beta,1} = 0$ and $p_1 = p_0$ (corresponding to an initial condition on the $x_{p_0}^\gamma$ limit cycle), we seek a sequence u_k and v_k for $k = 0, \ldots, \eta - 1$ that minimizes the cost function

$$
\begin{aligned}
J_1\big((u_k)_{k=0}^{\eta-1}, (v_k)_{k=0}^{\eta-1}\big) &= \sum_{k=0}^{\eta-1} u_k^2 + \sum_{k=0}^{\eta} \sum_{j=1}^{\beta} \alpha_{1,j}\psi_{j,k}^2 \\
&\quad + \alpha_2 \sum_{k=0}^{\eta} f_k(\theta_k),
\end{aligned}
\qquad (18)
$$

where $f_k(\theta)$ is a state-based penalty used to ensure that the phase reaches the prescribed target, and $\alpha_{1,1}, \ldots, \alpha_{1,\beta}$ and α_2 weight the relative importance of minimizing the overall energy of the input, achieving the control objective, and minimizing the value of the isostable coordinates– - recall that keeping the isostable coordinates small is necessary to ensure that the adaptive phase-isostable reduction (15) provides an accurate representation of the full model dynamics (4). It is possible to take $f_k(\theta_k) = 0$ for $k = 0, \ldots, \eta - 1$ to only consider the terminal value of θ for the phase based penalty, however, we allow for additional freedom in this state-based penalty to consider the intermediate values.

B. Problem formulation when using the nonadaptive phase-isostable reduction

When using the nonadaptive phase-isostable reduced order equation (9), the problem formulation is similar to the one given in Sec. III A, except that there is no adaptive parameter. We consider the difference equation

$$
\begin{aligned}
\theta_{k+1} &= [\omega(p_0) + Z(\theta_k, p_0) \cdot hu_k]\Delta t + \theta_k, \\
\psi_{j,k+1} &= [\kappa_j(p_0)\psi_{j,k} + I_j(\theta_k, p_0) \cdot hu_k]\Delta t + \psi_{j,k}, \\
&\quad j = 1, \ldots, \beta,
\end{aligned}
\qquad (19)
$$

where $u_k \in \mathcal{U}$. Letting $\theta_1 = \psi_{1,1} = \cdots = \psi_{\beta,1} = 0$ (corresponding to an initial condition on the $x_{p_0}^\gamma$ limit cycle), we seek a sequence u_k for $k = 0, \ldots, \eta - 1$ that minimizes the cost function:

$$J_2\big((u_k)_{k=0}^{\eta-1}\big) = \sum_{k=0}^{\eta-1} u_k^2 + \sum_{k=0}^{\eta} \sum_{j=1}^{\beta} \alpha_{1,j} \psi_{j,k}^2 + \alpha_2 \sum_{k=0}^{\eta} f_k(\theta_k). \tag{20}$$

Compared to the cost function (18), Eq. (20) does not consider an adaptive parameter. In this case, the dynamics (19) are simpler owing to the lower dimension, but there is less control over the isostable coordinate dynamics. This problem formulation can be viewed as a discrete time version of the control strategy considered in Ref. [28].

C. Problem formulation when using the phase-only reduction

The optimal control formulation becomes substantially simpler when using phase-only reduction (6) as compared to the formulations from Secs. III A or III B. Here, the relevant difference equation is

$$\theta_{k+1} = [\omega(p_0) + Z(\theta_k, p_0) \cdot h u_k] \Delta t + \theta_k, \tag{21}$$

where $u_k \in \mathcal{U}$. Letting $\theta_1 = 0$, we seek a sequence u_k for $k = 0, \ldots, \eta - 1$ that minimizes

$$J_3\big((u_k)_{k=0}^{\eta-1}\big) = \sum_{k=0}^{\eta-1} u_k^2 + \alpha_2 \sum_{k=0}^{\eta} f_k(\theta_k). \tag{22}$$

Without isostable coordinates, the cost function (22) only considers the trade-off between the phase-based penalty and the overall energy consumption. This problem formulation can be viewed as a discrete time version of the control strategy considered in [4].

D. Finding solutions of the optimal control problems

Optimal solutions of the cost functions from (18), (20), and (22) can be obtained computationally using the principle of optimality. Stated succinctly in Ref. [34], the principle of optimality states: "An optimal policy has the property that whatever the initial state and initial decisions are, the remaining decisions must constitute an optimal policy with regard to the state resulting from the first decision." This general principle allows for the computation of an optimal solution using a dynamic programming approach [34,35], dividing the larger problem into a smaller set of nested subproblems as described here. For instance, for the problem using the adaptive phase-isostable reduction (18), the update equations (17) can be written in shorthand notation according to

$$\chi_{k+1} = G(\chi_k, u_k, \nu_k), \tag{23}$$

where $k = 0, \ldots, \eta - 1$, where $\chi_k = [\theta_k, \psi_{1,k}, \ldots, \psi_{\beta,k}, p_k]^T$ is the state of the reduced order system and G is defined appropriately. Considering the cost function (18), one can also define a cost-to-go function:

$$J_{1,\eta-y}^*(\chi_{\eta-y}) = \begin{cases} \min_{\substack{u_k, \nu_k \\ \eta-y \leqslant k \leqslant \eta-1}} J_1\big((u_k)_{k=\eta-y}^{\eta-1}, (\nu_k)_{k=\eta-y}^{\eta-1}\big), & \text{if } y > 0 \\ \sum_{j=1}^{\beta} \alpha_{1,j} \psi_{j,\eta}^2 + \alpha_2 f_\eta(\theta_\eta), & \text{if } y = 0. \end{cases} \tag{24}$$

The cost-to-go function, which is a function of the state $\chi_{\eta-y}$, is the remaining cost when applying an optimal series of inputs, u_k and adaptive parameter updates, ν_k, over the final y time steps. Leveraging Bellman's principle of optimality [34], the cost-to-go function can be computed backwards in time according to

$$J_{1,\eta-y}^*(\chi_{\eta-y}) = \min_{\substack{u_{\eta-y} \subset \mathcal{U} \\ \nu_{\eta-y} \mid p_{\eta-y+1} \subset \mathcal{P}}} \left(u_{\eta-y}^2 + \sum_{j=1}^{\beta} \alpha_{1,j} \psi_{j,\eta-y}^2 + \alpha_2 f_{\eta-y}(\theta_{\eta-1}) + J_{\eta-y+1}^*(\chi_{\eta-y+1}) \right). \tag{25}$$

With knowledge of the cost-to-go function, the optimal inputs and parameter updates are given by

$$(u_k^*, \nu_k^*) = \operatorname*{argmin}_{\substack{u_k \subset \mathcal{U} \\ \nu_k \mid p_{\eta-y+1} \subset \mathcal{P}}} \left(u_k^2 + \sum_{j=1}^{\beta} \alpha_{1,j} \psi_{j,k}^2 + \alpha_2 f_k(\theta_k) + J_{1,k+1}^*(\chi_{k+1}) \right), \tag{26}$$

where χ_{k+1} is obtained according to the update rule (23). The optimal inputs u_k^* and ν_k^* can be computed according to (26) at all times $k = 0, \ldots, \eta - 1$ as a function of χ_k. Subsequent interpolation allows for the application of these inputs in the original differential equations.

The formulation of the cost functions in (18), (20), and (22) consider the control space $\mathcal{U}$ and the parameter update space $\mathcal{P}$ on a continuous domain. In practice, it is computationally infeasible to find the minimizer of (25) over a continuous set of inputs and parameter updates. Alternatively, computation

of the cost-to-go function in (25) can be performed by discretizing state space as well as the space of inputs and parameter updates and finding the minimizers u_{n-y} and ν_{n-y} over the resulting finite set of possibilities. Following this approach, solutions of the update rule (23) will generally not fall directly on a gridpoint necessitating interpolation at each step. Minimization of the cost functions J_2 and J_3, i.e., when using the nonadaptive phase-isostable reduced-order equations and the phase-only reduced-order equations can be performed using a similar strategy. When considering the

nonadaptive phase-isostable reduced-order equations there is no need to consider an adaptive parameter as part of the state. Similarly, the phase-only equations do not require an adaptive parameter or an isostable coordinate. This reduces the dimension of the problem which reduces the computational burden. However, the simpler reduced-order models do not always provide a good representation of the underlying system dynamics. These points are illustrated further in example problems considered in the next section.

IV. RESULTS

We apply the optimal control frameworks from Sec. III in two different numerical applications. For both models, the limit cycles are calculated using the interpolation with respect to p. For the first, we consider the problem of speeding up recovery from circadian misalignment caused by rapid travel through multiple time zones. For the second, we consider phase-based control of two strongly coupled neural oscillators.

A. Application to a circadian model in the context of a jet lag mitigation strategy

In mammals, the suprachiasmatic nucleus (SCN) is the master pacemaker for keeping circadian time. The SCN is comprised of a large population of coupled neurons [36,37] that maintain daily rhythms relative to a 24-hour light-dark cycle. Jet lag is caused by a mismatch between the environmental and circadian time [38] making the problem of rapidly shifting the phase of the circadian system (27) relevant in the context of jet-lag mitigation strategies. The suggested control approach hastens recovery from circadian misalignment by appropriately shifting the phase to account for travel across time zones. We investigate the adaptive phase-isostable reduction approach combined with a dynamic programming strategy to yield inputs that appropriately shift the phase. For small and intermediate inputs, both phase-only and phase-amplitude-based methods yield viable solutions. However, when it is necessary to apply large magnitude inputs, only the adaptive phase-amplitude strategy gives viable solutions.

Here we consider a simple model for $N = 10$ circadian oscillators originally proposed in Ref. [39]:

$$\dot{a}_i = h_1 \frac{K_1^n}{K_1^n + c_i^n} - h_2 \frac{a_i}{K_2 + a_i}$$
$$+ h_c \frac{KF(t)}{K_c + KF(t)} + S_i L(t) + p,$$
$$\dot{b}_i = h_3 a_i - h_4 \frac{b_i}{K_4 + b_i},$$
$$\dot{c}_i = h_5 b_i - h_6 \frac{c_i}{K_6 + c_i},$$
$$\dot{d}_i = h_7 a_i - h_8 \frac{d_i}{K_8 + d_i}. \tag{27}$$

for $i = 1, \ldots, N$. Above, the concentrations of the mRNA clock gene, its associated protein, and the nuclear form of the protein are represented by the variables a_i, b_i, and c_i, respectively, for cell i, d_i is a neurotransmitter that controls the

mean-field coupling $F(t)$, where $F(t) = (1/N) \sum_{j=1}^{N} d_j(t)$, and S_i is the sensitivity to light where $S_i = 1 + (i - 1)/45$, and $L(t)$ is an external light input. Constants are taken as $n = 7$, $h_1 = 1.05$, $h_2 = 0.525$, $h_c = 0.2$, $h_3 = 0.7$, $h_4 = 0.35$, $h_5 = 0.7$, $h_6 = 0.35$, $h_7 = 0.35$, $h_8 = 1$, $K_1 = 1$, $K_2 = 1$, $K_C = 1$, $K = 0.5$, $K_4 = 1$, $K_6 = 1$, $K_8 = 1$. Here, p is the adaptive parameter when considering the adaptive phase-isostable reduction strategy which yields stable limit cycles for $p \in [-0.01, 0.019]$ when taking $L(t) = 0$. When $L(t) = p = 0$, the period of the population oscillation is $T = 24.8$ hours. For the phase-only and nonadaptive phase-isostable reductions, p is taken to be 0. The collective oscillation exhibited by (27) has a total of 40 state variables. Parameters of (27) are identical to those from Fig. 1 of Ref. [39] except for n, h_1, h_2, and h_c which are modified made so that the period of the population oscillation when $p = 0$ is close to 24 h.

Using techniques described in Ref. [22], we numerically compute the necessary terms of the phase-only, nonadaptive phase-isostable, and adaptive phase-isostable reduced order equations. For each limit cycle parameterized by the constant value of p, $\theta(x, p) = 0$ corresponds to the moment that a_1 reaches its maximum value. As discussed in Ref. [40], due to symmetries that arise in (27), only three isostable coordinates are required to accurately capture the amplitude dynamics. The phase dynamics are taken to second-order accuracy in the expansion in isostable coordinates while the isostable coordinate dynamics are taken to first order accuracy. For instance, when considering the adaptive phase-isostable reduced order equations, the dynamics are

$$\dot{\theta} = \omega(p) + Z^T(\theta, p) U_e(t, p)$$
$$+ \sum_{k=1}^{3} \psi_k B^{k^T}(\theta, p) U_e(t, p) + D(\theta, p)\dot{p},$$
$$\dot{\psi}_j = \kappa_j(p)\psi_j + I_j^T(\theta, p) U(\theta, p) + Q_j(\theta, p)\dot{p},$$
$$j = 1, 2, 3, \tag{28}$$

where

$$U_e = [(S_1 L(t) - p) \; 0 \; 0 \; 0 \; (S_2 L(t) - p) \; \ldots$$
$$(S_N L(t) - p) \; 0 \; 0 \; 0]^T. \tag{29}$$

Note that the required terms of (28) are computed for a finite set of p-limit cycles so intermediate values can be obtained via interpolation. For the reduced order model (28), the θ coordinate corresponds to the phase of the limit cycle of the population oscillation, ψ_1 corresponds a mode associated with a spreading of the phases, and ψ_2 and ψ_3 are modes associated with a spreading of the oscillation amplitudes. Note that in Eq. (28), the second-order terms for the isostable coordinate dynamics do not improve the overall match between the full and reduced-order models and are simply truncated from the reduction. Equations (28) and (29) are used to inform the dynamics of the difference equation of the form (17) obtained using the forward Euler method with a time step of $\Delta t = 1$ h. We solve the associated optimization problem that minimizes the cost function (18) for different choices of target value, T_1
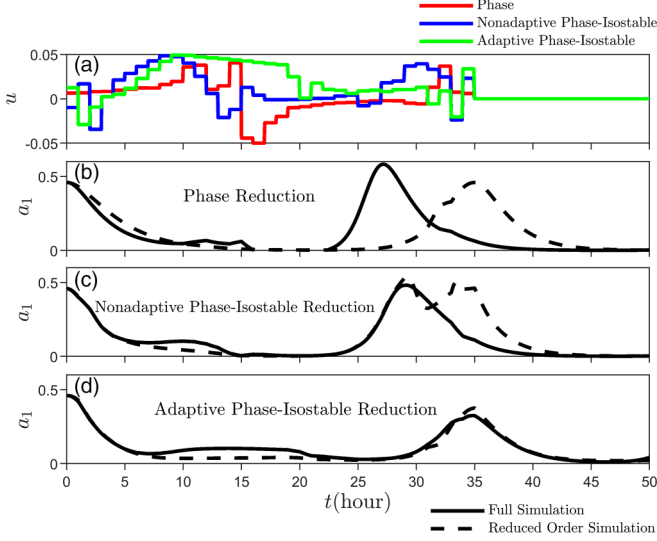
FIG. 1. When taking $T_1 = 35$ hours, (a) shows three optimal inputs obtained using three different representations for the reduced order dynamics. These inputs are applied to the full order models (27) in (b)–(d). Solid black lines show outputs from the full model while dashed lines show the predicted output from the relevant reduced order model. The output from the full model is substantially different from the output of the phase-only and nonadaptive phase-isostable reductions, ultimately yielding an input that does not achieve the control objective. The predictions between the full order model and the adaptive phase-isostable reduction are much closer; as such, the resulting optimal input does satisfy the control objective when applied to the full-order model.

FIG. 2. (a)–(e) State variables associated with the optimal solutions obtained with the adaptive and nonadaptive phase-isostable reductions when $T_1 = 35$ hours. While both reduced-order models satisfy $\theta(T_1) = 2\pi$, the ψ_1 coordinate when using the nonadaptive phase-isostable reduction is relatively large, degrading the accuracy of the reduced-order model and ultimately explaining the mismatch between the full-order and reduced-order models in (f). By contrast, the outputs from the full and adaptive phase-isostable reduced-order models in (g) are nearly identical and both satisfy the control objective.

subject to the constraints

$$-0.05 \leqslant u_k \leqslant 0.05,$$
$$-0.01 \leqslant p_k \leqslant 0.019,$$
$$-0.001 \leqslant v_k \leqslant 0.001. \qquad (30)$$

In (30), choosing an appropriately tight window on the feasible values of u_k, p_k, and v_k allows for a sufficiently fine discretization while limiting the computational burden. It is necessary to use different scaling factors $\alpha_{1,1}, \ldots, \alpha_{1,\beta}$ and α_2 for each choice of T_1. For instance, when $T_1 = 35$ hours, the values $\alpha_{1,1} = 2 \times 10^4$, $\alpha_{1,2} = 100$, $\alpha_{1,3} = 100$, and $\alpha_2 = 50$ are used. These scaling factors are chosen through trial and error so the control problem has a viable solution. With increasing T_1, we use increasing values of $\alpha_{1,1}$ with $\alpha_{1,2}$ and $\alpha_{1,3}$ remaining constant. We take

$$f_k(\theta_k) = 1 - \exp\left(-0.5(\theta_k - 2\pi)^2\right) \qquad (31)$$

as the state-based penalty.

Optimal inputs are also obtained using the nonadaptive phase-isostable and phase-only reductions using the strategy described in Secs. III B and III C, respectively. For this optimization, we consider the same constraint on the input from Eq. (30); additionally phase-only and nonadaptive phase-isostable reductions from (6) and (9), respectively, are computed for the limit cycle that results when taking $L_0 = 0$.

Figure 1 shows results when considering the control problem taking $T_1 = 35$ hours, i.e., so the period is increased

by about 10 h. Figure 1(a) shows three different optimal inputs obtained from minimizing the three different cost functions (18), (20), and (22) that result when using the adaptive phase-isostable, nonadaptive phase-isostable, and phase-only representations for the reduce order dynamics. Note that while these inputs are substantially different, they all satisfy $\theta(T_1) = 2\pi$ for their respective difference equations. Their efficacy when applied to the full model (27) is not the same, however, as shown from the black traces Figs. 1(b)– 1(d). Both inputs obtained from phase-only and nonadaptive phase-isostable reduction yield periods that are less than the target. The input obtained using the adaptive phase-isostable reduction yields an input that achieves the intended goal.

Considering the optimal control inputs that were shown in Fig. 1, Figs. 2(a)–2(e) show the value of the state variables associated with the optimal solution obtained when considering the adaptive phase-isostable reduction (blue lines) and the nonadaptive phase-isostable reduction (green lines). As seen in Fig. 2(a), both solutions reach $\theta = 2\pi$ at $t = 35$ hours. While both of these methods penalize against large magnitude isostable coordinates, $\max_t(|\psi_1|, |\psi_2|, |\psi_3|) = 1.3$ for the nonadaptive phase-isostable approach while $\max_t(|\psi_1|, |\psi_2|, |\psi_3|) = 0.6$ when using the adaptive phase-isostable reduction approach. The difference in the magnitude of the isostable coordinates explains the difference in the effectiveness of the resulting control input when it is applied to the full model equations (27), shown once again in panels (f) and (g) for reference.

Figure 3 collects results for different values of T_1. Here, we define T_a to be the actual time required to complete a
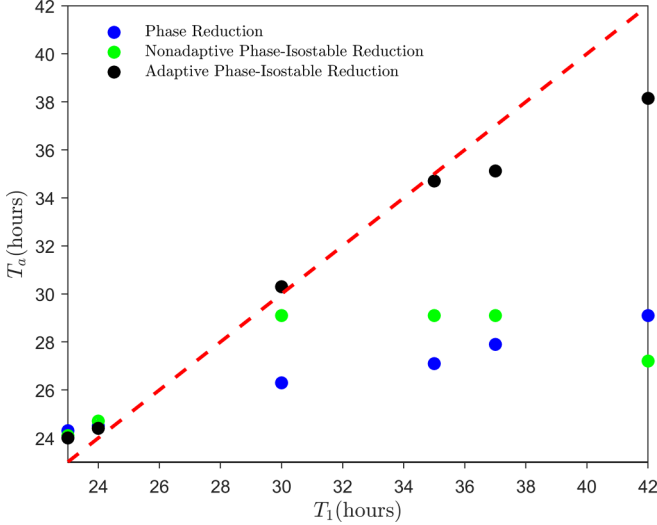
FIG. 3. Optimal inputs for various choices of T_1 are obtained by solving cost functions (18), (20), and (22) and applied to the full-order model (27). Each dot represents the results for a single input, T_a is the actual oscillation period when the resulting input is applied to the full model. If there is perfect agreement between the full and reduced order models, the dot will fall on the dashed red identity line, which is shown for reference. As the difference between T_1 and the unperturbed period $T = 24.8$ h begins to increase, larger magnitude inputs are required necessitating the use of more accurate methods to accurately handle the amplitude dynamics. The nonadaptive phase-isostable reduction method generally outperforms the phase-only reduction, however, the adaptive phase-isostable reduction is superior to both, especially for larger values of T_1.

full oscillation when the input obtained taking the target T_1 is applied to the full order model (27). Each dot in Fig. 3 represents the result of a single trial—if there is a perfect match between the full-order and reduced-order models, the dot will fall on the dashed red identity line. Mismatch between the reduced- and full-order models will degrade the efficacy of the resulting control input. We find that when using the adaptive phase-isostable reduction to solve the control problem, the resulting optimal input achieves the desired oscillation time for T_1 up to 35 h. After this point, there is a slight degradation. By contrast, efficacy of the optimal inputs obtained using the phase-only and nonadaptive phase-isostable reduced-order model begin to degrade much earlier.

B. Application to a model of strongly coupled neurons

Here, we consider a prototype problem of phase-based control of two strongly coupled neural oscillators. The model equations are taken from Ref. [41],

$$C_m \dot{v}_j = -I_L(v_j) - I_{Na}(v_j, h_j) - I_K(v_j, h_j) - I_T(v_j, r_j)$$

$$+ I_b + a(v_i - v_j) + \frac{j}{2}u(t) + p,$$

$$\dot{h}_j = \frac{h_\infty - h}{\tau_h},$$

$$\dot{r}_j = \frac{r_\infty - r}{\tau_r}, \tag{32}$$

where $j = 1, 2$ and $i = 2, 1$. Here v_j is the transmembrane voltage of neuron j, h_j and r_j are associated gating variables, I_L, I_{Na}, I_K, and I_T are ionic currents, $I_b = 8 \mu A/\mu F$ is a constant baseline current, $u(t)$ is an external current, and $C_m = 1$ $\mu F/cm^2$ is the membrane capacitance. Here, the influence of $u(t)$ is reduced by a factor 2 for neuron 1. Electronic coupling is added to the voltage equation [42], where $a = 2$ sets the coupling strength. Auxiliary functions and constants are given below: $h_\infty = 1/(1 + \exp((v + 41)/4))$, $r_\infty = 1/(1 + \exp((v + 84)/4))$, $\alpha_h = 0.128 \exp(-(v + 46)/18)$, $\beta_h = 4/(1 + \exp(-(v + 23)/5))$, $\tau_h = 1/(\alpha_h + \beta_h)$, $\tau_r = (28 + \exp(-(v + 25)/10.5))$, $m_\infty = 1/(1 + \exp(-(v + 37)/7))$, $p_\infty = 1/(1 + \exp(-(v + 60)/6.2))$, $I_L = g_L(v - e_L)$, $I_{Na} = g_{Na}(m_\infty^3)h(v - e_{Na})$, $I_K = g_K((0.75(1 - h))^4)(v - e_K)$, $I_T = g_T(p_\infty^2)r(v - e_T)$, $g_L = 0.05 \, mS/m^2$, $e_L = -70 \, mV$, $g_{Na} = 3 \, mS/m^2$, $e_{Na} = 50 \, mV$, $g_K = 5 \, mS/m^2$, $e_K = -90 \, mV$, $g_T = 5 \, mS/m^2$, $e_T = 0 \, mV$.

When evaluating the adaptive phase-isostable reduction technique, p is taken as the adaptive parameter yielding stable limit cycles for $p \in [-9.3, 8.1] \mu A/\mu F$ when $u(t) = 0$. When $u(t) = p = 0$, the aggregate oscillation has a period of $T = 6.56$ ms. p is taken to be 0 for phase-only and nonadaptive phase-isostable reductions. For each limit cycle parameterized by a constant value of p, $\theta(x, p) = 0$ corresponds to the point at which v_1 reaches its maximum value. We numerically evaluate the required terms of the phase-only, nonadaptive phase-isostable, and adaptive phase-isostable reduced order equations using approaches described in [22]. For example, while considering the adaptive phase-isostable reduced order equations, the dynamics are

$$\dot{\theta} = \omega(p) + Z^T(\theta, p)U_e(t, p) + D(\theta, p)\dot{p},$$

$$\dot{\psi}_j = \kappa_j(p)\psi_j + I_j^T(\theta, p)U_e(t, p) + Q_j(\theta, p)\dot{p},$$

$$j = 1, 2, 3, \tag{33}$$

where

$$U_e = \begin{bmatrix} (u(t)/2 - p) & 0 & 0 & (u(t) - p) & 0 & 0 \end{bmatrix}^T. \tag{34}$$

Equations (33) and (34) are used to inform the dynamics of the difference equation of the form (17) obtained using the forward Euler method with a time step of $\Delta t = 0.5$ ms. We solve the optimization problem that minimizes the cost function (18) for various target values, T_1 subject to constraints

$$-11 \leqslant u_k \leqslant 11,$$

$$-9.3 \leqslant p_k \leqslant 8.1, \tag{35}$$

$$-1.1 \leqslant v_k \leqslant 1.1.$$

In (35), choosing an appropriately tight window on the feasible values of u_k, p_k and v_k allows for a sufficiently fine discretization while limiting the computational burden.

For this example, we consider only an endpoint cost for the state-based penalty:

$$f_k(\theta_k) = \begin{cases} 0, & \text{if } k = 0 \\ 1 - \exp(-0.5(\theta_k - 2\pi)^2), & \text{if } k = \eta. \end{cases} \tag{36}$$

For each T_1, distinct scaling factors $\alpha_{1,1}, \ldots, \alpha_{1,\beta}$ and α_2 are used. For example, when $T_1 = 7.5$ ms, the values $\alpha_{1,1} = 1$, $\alpha_{1,2} = 0.01$, $\alpha_{1,3} = 10$, and $\alpha_2 = 8 \times 10^7$ are considered.
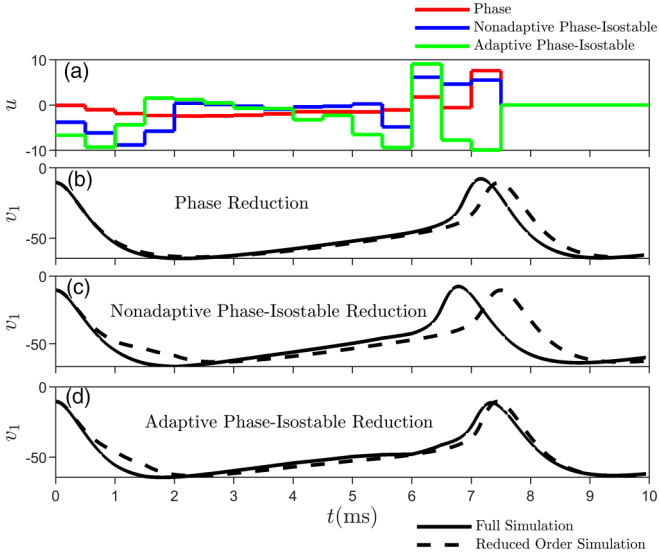
FIG. 4. When taking $T_1 = 7.5$ ms, (a) shows three optimal inputs obtained using three different representations for the reduced order dynamics. These inputs are applied to the full order models (32) in (b-d). Solid lines show outputs from the full model while dashed lines show the output predicted by the relevant reduced order model. The output from the full order model is substantially different from the output of the phase-only and nonadaptive phase-isostable reductions, ultimately yielding an input that does not achieve the control objective. By contrast, the output from the full and adaptive phase-isostable reduced order models in (d) are nearly identical with both satisfying the control objective.

Optimal inputs are also obtained utilizing the nonadaptive phase-isostable and phase-only reduction strategies described in Sections III B and III C, respectively.

Figure 4 shows results when considering the spike timing control problem taking $T_1 = 7.5$ ms, i.e., increasing the period by around 1 ms. (a) shows three different optimal inputs obtained by minimizing the three cost functions (18), (20), and (22) that use the adaptive phase-isostable, nonadaptive phase-isostable, and phase-only representations, respectively, for the reduction order dynamics. While these inputs differ significantly, they all satisfy $\theta(T_1) = 2\pi$ for their respective difference equations. Their efficacy when applied to the underlying model (32) is substantially different, as evidenced by the black traces in (b)–(d). Both phase-only and nonadaptive phase-isostable reduction inputs produce periods shorter than the target.

Using the optimal control inputs shown in Fig. 4, (a)–(e) of Fig. 5 show the value of the state variables associated with the optimal solution obtained when considering the adaptive phase-isostable reduction (blue lines) and the nonadaptive phase-isostable reduction (green lines). As seen in Fig. 5(a), both solutions reach $\theta = 2\pi$ at the target $t = 7.5$ ms. While both approaches penalize for large magnitude isostable coordinates, $\max_t(|\psi_1|, |\psi_2|, |\psi_3|) = 8.7$ for the nonadaptive phase-isostable reduction approach and $\max_t(|\psi_1|, |\psi_2|, |\psi_3|) = 2.4$ for the adaptive phase-isostable reduction approach. The difference in the magnitude of the isostable coordinates explains the difference in the efficacy of the resultant control input when applied to the
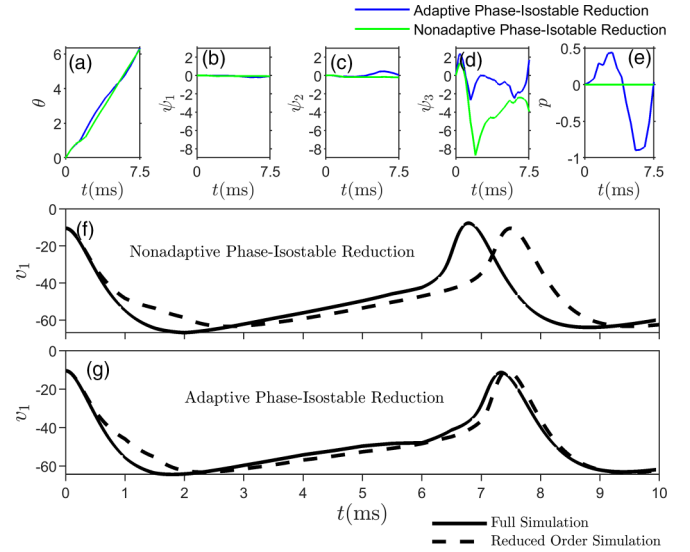
FIG. 5. (a-e) show the state variables associated with the optimal solutions obtained with the adaptive and nonadaptive phase-isostable reductions when taking $T_1 = 7.5$ ms. While both reduced order models satisfy $\theta(T_1) = 2\pi$, the ψ_3 coordinate when using the nonadaptive phase-isostable reduction is relatively high, degrading the accuracy of the reduced order model and ultimately explaining mismatch between the full order and reduced order models in (f). By contrast, the results from the full and reduced order models in (g) are nearly identical and both satisfy the control objective.

entire model equations (32), as illustrated in (f) and (g) for reference.

Figure 6 shows the results for various T_1 values. T_a is defined here as the actual time necessary to complete a full oscillation when the input obtained using the target T_1 is applied to the full order model (32). Each dot in Fig. 6 represents the outcome of a single trial; if there is a perfect match between the full order and reduced order models, the dot will fall on the dashed red identity line. Mismatches between the reduced and full order models will diminish the efficacy of the resulting control input. When the control problem is solved using the adaptive phase-isostable reduction, the resulting optimal input achieves the requisite oscillation time for T_1 up to 12 ms. There is a small degradation after this point. The efficacy of optimal inputs obtained using the phase-only and nonadaptive phase-isostable reduced order models, on the other hand, begins to degrade significantly earlier.

V. CONCLUSION AND DISCUSSION

Phase reduction is an essential tool that can be used to understand and control the behavior of weakly perturbed limit cycle oscillators. In situations that require strong perturbation, i.e., those that drive the dynamics far from the underlying limit cycle, additional information about the amplitude dynamics must be considered. Here we consider the adaptive phase-isostable reduction approach in conjunction with a dynamic programming strategy to implement phase-based control of limit cycle oscillators in a strongly perturbed regime. Considering the results presented in Sec. IV, the proposed approach yields inputs that are substantially more accurate than other
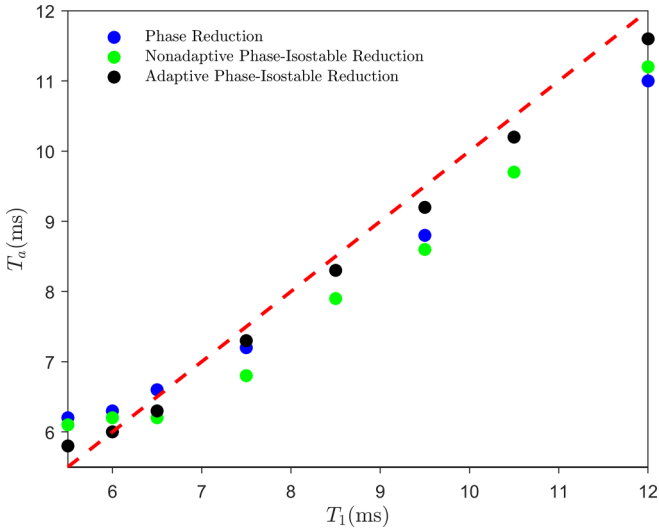
FIG. 6. Optimal inputs obtained for various choices of T_1 are obtained by solving cost functions (18), (20), and (22) and applied to the full order model (32). Each dot compares T_1 (the target oscillation period) to T_a (the actual oscillation period when the input is applied to the full model). For a perfect agreement between the full and reduced order models, the dot will fall on the dashed red identity line, shown for reference. Note that the unperturbed period is $T = 6.46$ ms. As the difference between T_1 and T begins to increase, more accurate methods are required to accurately handle the amplitude dynamics. The nonadaptive phase-isostable reduction method gives results that outperform the phase-only reduction, however the adaptive phase-isostable reduction is superior to both, especially for larger values of T_1.

reduced order modeling and control strategies when large magnitude inputs must be used.

In the weakly perturbed setting, phase-only reduction strategies [1–3] can be used, requiring a single phase variable to represent the underlying N-dimensional system. References [28,27,32] augment the phase dynamics with information about amplitude dynamics using an isostable coordinate system, yielding control inputs that outperform phase-only models when moderately sized inputs are used. The adaptive phase-isostable strategy used here takes this analysis a step further, considering a continuous family of limit cycles in the reduction that can accurately accommodate even larger magnitude inputs.

This work highlights an essential trade-off when considering reduced order modeling of strongly perturbed limit cycle oscillators. Specifically, as stronger inputs are required, more accurate information about the amplitude dynamics are necessary so that the reduced order model remains an accurate reflection of the full order dynamics. This additional information generally results in additional dimensions and degrees of freedom in the reduced order models. In the models considered in this work, the phase-only, nonadaptive phase-isostable, and adaptive phase-isostable models required 1 (phase), 4 (phase and three isostable coordinates), and 5 (phase, three isostable coordinates, and adaptive parameter) dimensions respectively, with each additional dimension increasing the computational expense of finding an optimal solution to the associated control problem. Additionally, the optimization

when using adaptive phase-isostable reduction (18) has two degrees of freedom (the change in the adaptive parameter and the control input) while the other two cost functions only consider the input at each timestep. For the formulation and solution of general phase-based control problems, we recommend starting with a phase-only reduction. If phase-only reduction proves insufficient, we recommend moving to nonadaptive phase-isostable reduction and finally adaptive phase-isostable reduction strategies as necessary.

While the adaptive phase-amplitude reduction strategy provides a more accurate representation of the underlying model as compared to the phase-only or nonadaptive phase-isostable reduction, it generally does not provide a perfect match. As such, care must still be taken in the design of the cost functions associated with a given control problem. For example, in the application from Section IV A, the state-based penalty from (31) is applied at each timestep. For this same example, we also considered a state-based penalty applied only at the endpoint [similar to the penalty from Eq. (36)], but the resulting control yielded inputs that attempted to rapidly shift the phase in the final moments of the interval $t \in [0, T_1]$. When these inputs were subsequently applied to the full order model (27), the results did not match those of the reduced order model. Instead, considering the state-based penalty at each timestep ultimately yielded control inputs for which the behavior of full order and adaptive phase-amplitude reduction strategies matched. We emphasize that modifications to the cost function did not yield viable solutions when using the phase-only or nonadaptive phase-isostable reductions in either of the applications considered in this work.

We note that there is no guarantee that an adequate solution for a given control problem exists. In both applications considered in this work, none of the methods could find a viable solution when choosing the target T_1 to be much smaller than the unperturbed period. Of course, each method is able to find solutions to optimize the associated cost function but in the case of the phase-only reduction the resulting input did not work when applied to the full order model. In the case of the phase-amplitude reduction, the optimal solution was to apply input with very small magnitude indicating that the state-based penalty cannot be mitigated and that the next best thing is to do nothing. It may be the case that no inputs will yield a full oscillation for smaller values of T_1 for each of the models considered in this work. It would be of interest to investigate the fundamental limitations of the models themselves to more carefully address this question.

In this work, we only consider a single control objective of modifying the period of a general limit cycle oscillator with external input. However, we believe that the insight gained from this study would readily extend to other phase-based control problems (e.g., that consider desynchronization, etc.) Owing to the low dimensionality of phase-only reduction, it is generally the best option when applicable, allowing for more sophisticated control and analysis techniques. When required perturbations are strong enough that phase-only reduction is not a possibility, information about the amplitude coordinates must be considered. While there are many options available to consider the amplitude dynamics, a judicious choice is necessary in order to obtain a model that is not prohibitively high-dimensional but still accurately reflects the full model

dynamics. Our results indicate that adaptive phase-isostable reduced order models may be well-suited for this task and further investigation about how best to choose the adaptive parameter set as well as the parameter update function would be warranted.

[1] A. Winfree, *The Geometry of Biological Time*, 2nd ed. (Springer Verlag, New York, 2001).

[2] G. B. Ermentrout and D. H. Terman, *Mathematical Foundations of Neuroscience* (Springer, New York, 2010), Vol. 35.

[3] Y. Kuramoto, *Chemical Oscillations, Waves, and Turbulence* (Springer-Verlag, Berlin, 1984).

[4] J. Moehlis, E. Shea-Brown, and H. Rabitz, Optimal inputs for phase models of spiking neurons, ASME J. Comput. Nonlinear Dyn. **1**, 358 (2006).

[5] A. Zlotnik, Y. Chen, I. Z. Kiss, H. A. Tanaka, and J. S. Li, Optimal waveform for fast entrainment of weakly forced nonlinear oscillators, Phys. Rev. Lett. **111**, 024102 (2013).

[6] D. Wilson and J. Moehlis, Optimal chaotic desynchronization for neural populations, SIAM J. Appl. Dynamical Syst. **13**, 276 (2014).

[7] S. H. Strogatz, D. M. Abrams, A. McRobie, B. Eckhardt, and E. Ott, Crowd synchrony on the Millennium Bridge, Nature (London) **438**, 43 (2005).

[8] F. Dörfler, M. Chertkov, and F. Bullo, Synchronization in complex oscillator networks and smart grids, Proc. Natl. Acad. Sci. **110**, 2005 (2013).

[9] D. M. Abrams and S. H. Strogatz, Chimera states for coupled oscillators, Phys. Rev. Lett. **93**, 174102 (2004).

[10] D. Wilson and J. Moehlis, Clustered desynchronization from high-frequency deep brain stimulation, PLoS Comput. Biol. **11**, e1004673 (2015).

[11] J. Guckenheimer and P. Holmes, *Nonlinear Oscillations, Dynamical Systems, and Bifurcations of Vector Fields* (Springer Verlag, New York, 1983), Vol. 42.

[12] R. Snari, M. R. Tinsley, D. Wilson, S. Faramarzi, T. I. Netoff, J. Moehlis, and K. Showalter, Desynchronization of stochastically synchronized chemical oscillators, Chaos **25**, 123116 (2015).

[13] C. O. Diekman and A. Bose, Entrainment maps: a new tool for understanding properties of circadian oscillator models, J. Biol. Rhythms **31**, 598 (2016).

[14] J. Cui, C. C. Canavier, and R. J. Butera, Functional phase response curves: A method for understanding synchronization of adapting neurons, J. Neurophysiol. **102**, 387 (2009).

[15] J. Foss and J. Milton, Multistability in recurrent neural loops arising from delay, J. Neurophysiol. **84**, 975 (2000).

[16] T. I. Netoff, C. D. Acker, J. C. Bettencourt, and J. A. White, Beyond two-cell networks: Experimental measurement of neuronal responses to multiple synaptic inputs, J. Comput. Neurosci. **18**, 287 (2005).

[17] W. Kurebayashi, S. Shirasaka, and H. Nakao, Phase reduction method for strongly perturbed limit cycle oscillators, Phys. Rev. Lett. **111**, 214101 (2013).

[18] Y. Park and B. Ermentrout, Weakly coupled oscillators in a slowly varying world, J. Comput. Neurosci. **40**, 269 (2016).

[19] K. Pyragas and V. Novičenko, Phase reduction of a limit cycle oscillator perturbed by a strong amplitude-modulated high-frequency force, Phys. Rev. E **92**, 012910 (2015).

[20] M. Rosenblum and A. Pikovsky, Numerical phase reduction beyond the first order approximation, Chaos **29**, 011105 (2019).

[21] D. Wilson and B. Ermentrout, Phase models beyond weak coupling, Phys. Rev. Lett. **123**, 164101 (2019).

[22] D. Wilson, Phase-amplitude reduction far beyond the weakly perturbed paradigm, Phys. Rev. E **101**, 022220 (2020).

[23] D. Takeshita and R. Feres, Higher order approximation of isochrons, Nonlinearity **23**, 1303 (2010).

[24] I. Mezić, Spectrum of the Koopman operator, spectral expansions in functional spaces, and state-space geometry, J. Nonlinear Sci. **30**, 2091 (2020).

[25] M. D. Kvalheim and S. Revzen, Existence and uniqueness of global Koopman eigenfunctions for stable fixed points and periodic orbits, Physica D **425**, 132959 (2021).

[26] D. Wilson and J. Moehlis, Isostable reduction of periodic orbits, Phys. Rev. E **94**, 052213 (2016).

[27] S. Takata, Y. Kato, and H. Nakao, Fast optimal entrainment of limit-cycle oscillators by strong periodic inputs via phase-amplitude reduction and Floquet theory, Chaos **31**, 093124 (2021).

[28] B. Monga and J. Moehlis, Optimal phase control of biological oscillators using augmented phase reduction, Biol. Cybern. **113**, 161 (2019).

[29] D. Wilson, An adaptive phase-amplitude reduction framework without $\mathcal{O}(\epsilon)$ constraints on inputs, SIAM J. Appl. Dyn. Syst. **21**, 204 (2022).

[30] J. Guckenheimer, Isochrons and phaseless sets, J. Math. Biology **1**, 259 (1975).

[31] D. Jordan and P. Smith, *Nonlinear Ordinary Differential Equations: An Introduction for Scientists and Engineers* (Oxford University Press, Oxford, 2007), Vol. 10.

[32] D. Wilson and B. Ermentrout, Greater accuracy and broadened applicability of phase reduction using isostable coordinates, J. Math. Biol. **76**, 37 (2018).

[33] B. Pietras and A. Daffertshofer, Network dynamics of coupled oscillators and phase reduction techniques, Phys. Rep. **819**, 1 (2019).

[34] R. E. Bellman and S. E. Dreyfus, *Applied Dynamic Programming* (Princeton University Press, Princeton, NJ, 1962).

[35] D. Kirk, *Optimal Control Theory* (Dover Publications, New York, 1998).

[36] R. Y. Moore, J. C. Speh, and R. K. Leak, Suprachiasmatic nucleus organization, Cell Tissue Res. **309**, 89 (2002).

[37] S. M. Reppert and D. R. Weaver, Coordination of circadian timing in mammals, Nature (London) **418**, 935 (2002).

[38] R. L. Sack Jr, D. Auckley, R. R. Auger, M. A. Carskadon, K. P. Wright, Jr., M. V. Vitiello, and I. V. Zhdanova, Circadian rhythm sleep disorders: Part I, basic principles, shift work and jet lag disorders, Sleep **30**, 1460 (2007).

[39] D. Gonze, S. Bernard, C. Waltermann, A. Kramer, and H. Herzel, Spontaneous synchronization of coupled circadian oscillators, Biophys. J. **89**, 120 (2005).

[40] D. Wilson and B. Ermentrout, Augmented phase reduction of (not so) weakly perturbed coupled oscillators, SIAM Rev. **61**, 277 (2019).

[41] J. Rubin and D. Terman, High frequency stimulation of the subthalamic nucleus eliminates pathological thalamic rhythmicity in a computational model, J. Comput. Neurosci. **16**, 211 (2004).

[42] D. Johnston and S. M. Wu, *Foundations of Cellular Neurophysiology* (MIT Press, Cambridge, MA, 1994).